

## Supporting Information

### ZnO@ABS/TPU/CaSiO<sub>3</sub> 3D Skeleton and Its Adsorption/Photocatalysis

#### Properties for Dye Contaminants Removal

Mengli Zhang<sup>a,b,1</sup>, Xinshu Xia<sup>b,c,\*</sup>, Changlin Cao<sup>b,c</sup>, Hun Xue<sup>a,c</sup>, Yujin Yang<sup>b,c</sup>, Wei Li<sup>b,c</sup>, Qinghua

Chen<sup>b,d</sup>, Liren Xiao<sup>a,b\*</sup>, Qingrong Qian<sup>b,c\*</sup>

a. College of Chemistry and Materials Science, Fujian Normal University, Fuzhou, Fujian 350007, China.

b. Engineering Research Center of Polymer Green Recycling of Ministry of Education, Fujian Normal University, Fuzhou, Fujian 350007, China.

c. College of Environmental Science and Engineering, Fujian Normal University, Fuzhou, Fujian 350007, China.

d. Fuqing Branch, Fujian Normal University, Fuzhou 350007, China.

**Corresponding author at:** Corresponding author at: College of Environmental Science and Engineering, Fujian Normal University, Fuzhou 350007, China (Q.-R. Qian). College of Chemistry and Materials Science, Fujian Normal University, Fuzhou 350007, China (L.-R. Xiao). Engineering Research Center of Polymer Green Recycling of Ministry of Education, Fuzhou 350007, China (X.-S. Xia).

E-mail address: qrqian@fjnu.edu.cn (Q.-R. Qian), xlr1966@fjnu.edu.cn (L.-R. Xiao),

xsxia@fjnu.edu.cn (X.-S. Xia).

## 1、Ca<sup>2+</sup> doped ZnO

Fig. S1 shows SEM and XRD patterns of different concentration of Ca doping on the basis of the experimental conditions of ZnO synthesis in this experiment. In the figure, it can be clearly found that the morphology of ZnO grown on the 3D backbone is quite different from that grown under the experimental conditions. Due to the hydrophilicity of the backbone itself and the different Ca<sup>2+</sup> concentration, an environment conducive to the growth of nanospheres with larger specific surface area is formed near the skeleton on the basis of the original experimental conditions. It can be seen from Fig. 1 SEM that the morphology of ZnO crystal changes gradually with the increase of Ca<sup>2+</sup> concentration. When the concentration of Ca<sup>2+</sup> is more than 10 mol%, the morphology of ZnO crystal grows from flat to spherical. The XRD pattern shows that with the increase of Ca<sup>2+</sup> doping concentration, the peak of XRD first moved slightly to the lower  $2\theta$  direction and then gradually moved to the higher  $2\theta$  direction. Compared with the XRD peak in the text, it was found that the XRD peak in the text shifted slightly to the lower  $2\theta$  direction, and there were indeed Ca<sup>2+</sup> mixed and the concentration was between 1-15 mol%, which was conducive to the formation of small nanosphere ZnO on the 3D backbone surface.

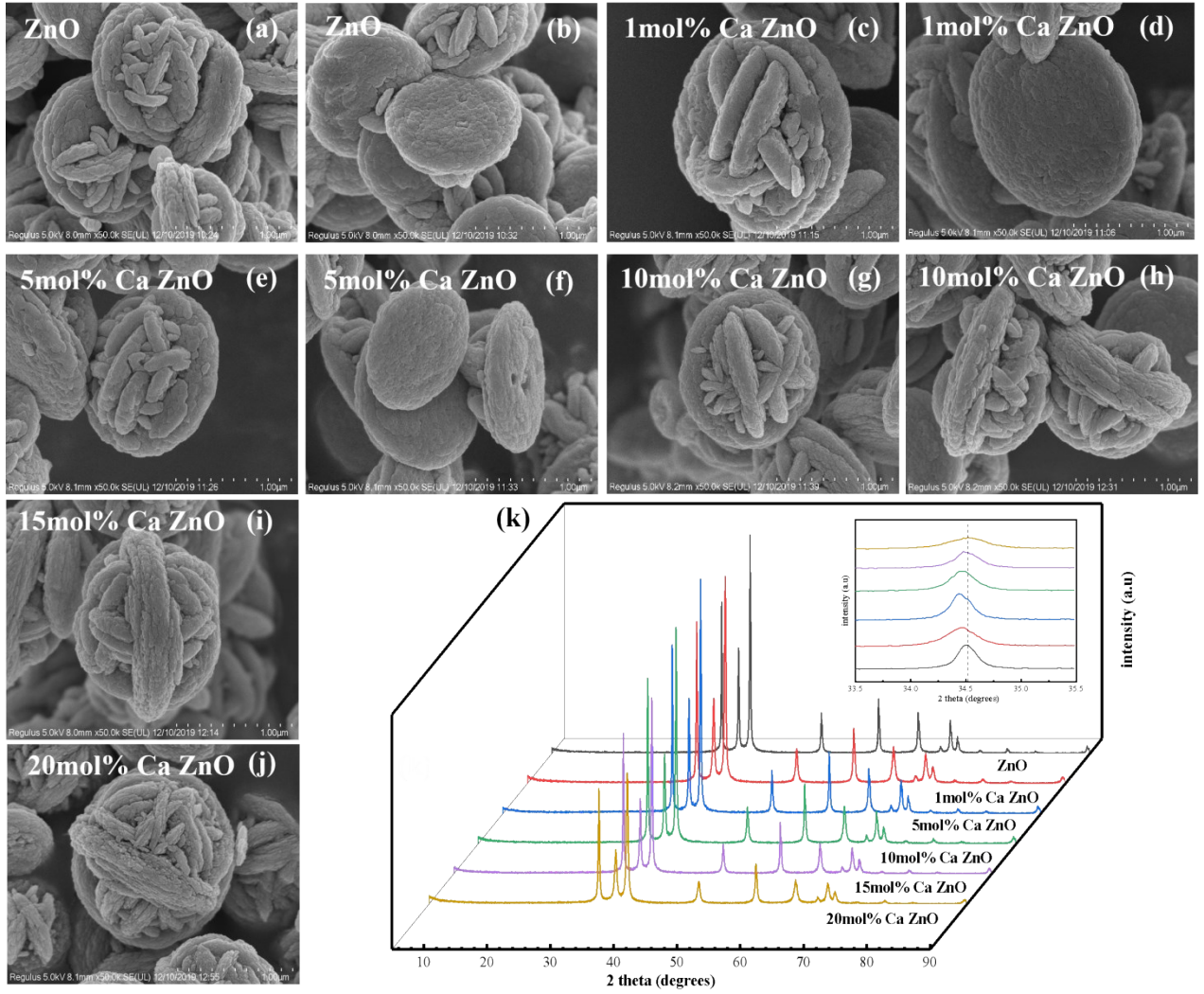


Fig.S1. SEM images of ZnO doped with different calcium ion concentrations: (a), (b)0 mol%; (c), (d) 1 mmol%; (e), (f)5 mol%; (g), (h)10 mol%; (i)15 mol%; (j)20 mol%; (k) XRD peaks of different samples.

## 2、Adsorption kinetics fitting

Several kinetic models were used to study the adsorption mechanism of RhB. They are pseudo-first-order kinetic model, pseudo-second-order kinetic model and intra-particle diffusion model. The formulas are as follows:

Pseudo-first-order kinetic model equations: 
$$\ln(q_e - q_t) = \ln q_e - k_1 t \quad (3)$$

pseudo-second-order kinetic model equations: 
$$\frac{t}{q_t} = \frac{1}{k_2 q_e^2} + \frac{t}{q_e} \quad (4)$$

intra-particle diffusion model equations: 
$$q_t = k_{id} t^{1/2} + C \quad (5)$$

Where  $q_e$  ( $\text{mg}\cdot\text{g}^{-1}$ ) is the adsorption amount of the adsorbent when the solution reaches the adsorption equilibrium,  $q_t$  ( $\text{mg}\cdot\text{g}^{-1}$ ) is the adsorption amount of the adsorbent at a certain time, and  $k_1$  and  $k_2$  are the adsorption equilibrium rate constants.  $K_{id}$  ( $\text{mg}\cdot\text{g}^{-1}\cdot\text{h}^{1/2}$ ) is the internal diffusion rate constant at different stages,  $i$  is a different stage, and the magnitude of  $C$  value reflects the thickness of the boundary layer.

The pseudo-first-order kinetics usually refers to the kinetics of the reaction rate determined by only one factor. The pseudo-second-order kinetics assumes that a chemical reaction occurs in the adsorption process, or that there is electron sharing or electron transfer occurs between the adsorbate and the adsorbent, which provides the best correlation adsorption mechanism. It can be seen from (a), (b) in Fig. S2 and Table S1 that the correlation coefficient after fitting the pseudo-second-order kinetic model is higher than that of the pseudo-first-order kinetic model and the calculated adsorption capacity ( $q_e$ , cal) of the pseudo-second-order model is more consistent with the experimental adsorption capacity ( $q_e$ , exp). Therefore, the pseudo second-order kinetic model is more suitable for the adsorption of RhB by ZnO-ATC and ATC adsorbents. By referring to the literature, it can be concluded that chemical adsorption is the main process, which is caused by exchange valence and electron transfer between adsorbate and adsorbent.

In order to further study the adsorption mechanism of RhB by backbone, the adsorption process of the chemisorbed heterogeneous adsorbent was further explained by intraparticle diffusion. From fig. S2(c), (d) and 3, it can be seen that the correlation coefficients of the intraparticle diffusion model are larger than 0.97, which indicates that the intraparticle diffusion model is suitable for the

adsorption process. As can be seen, there are two steps in the curve, the first part represents instantaneous or external surface adsorption, which is due to high initial RhB concentration and a large number of active adsorption sites. In the second part, the decrease in the adsorption rate is considered to be gradually slow adsorption until the equilibrium stage, and the intraparticle diffusion is further slowed down because the residual RhB concentration in the solution gradually decreases to a very low level. In addition, the figure does not go through the origin, indicating that the adsorption process is controlled by multiple adsorption steps, and is divided into three stages. In the first stage, RhB<sup>+</sup> migrates to the surface of the backbone under electrostatic traction. In the second stage, RhB<sup>+</sup> moves into the pores and adsorbs to the internal position of the adsorbent, which is called intraparticle diffusion. In the third stage, RhB diffuses through smaller pores, called inter-particle diffusion.

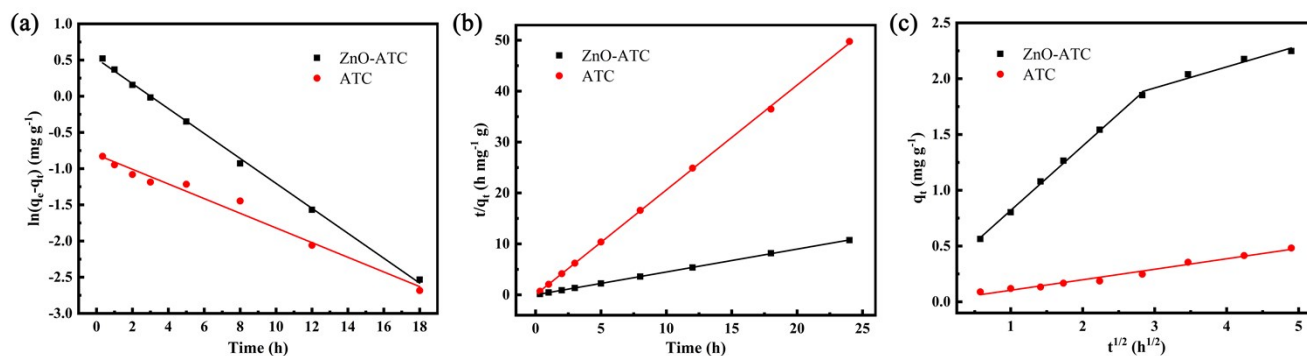


**Fig.S2.** Fitting curves by (a)the pseudo-first-order,(b)pseudo-second-order and (c)intra-particle diffusion for RhB adsorption onto different samples

**Table.S2.** Kinetic parameters for pseudo-first-order, pseudo-second-order models and intra-particle diffusion

Sample	$q_e$ , $\text{mg g}^{-1}$	Pseudo-first-order			Pseudo-second-order			Intra-particle diffusion			
		$k_1/(\text{h}^{-1})$	$q_e/(\text{mg} \cdot \text{g}^{-1})$	$R^2$	$K_2(\text{g} \cdot \text{mg}^{-1} \cdot \text{h}^{-1})$	$q_e(\text{mg} \cdot \text{g}^{-1})$	$R^2$	$K_{1d}(\text{mg} \cdot \text{g}^{-1} \cdot \text{h}^{1/2})$	$R^2$	$K_{2d}(\text{mg} \cdot \text{g}^{-1} \cdot \text{h}^{1/2})$	$R^2$
Zn-ATC	2.248	0.172	1.714	0.997	0.449	2.237	0.998	0.578	0.998	0.189	0.941
ATC	0.487	0.101	0.414	0.980	0.168	0.482	0.996	0.094	0.975	–	–